

Searching for Extrasolar Planets in the Gravitational Microlensing Event MB10311

A Senior Honors Thesis

Presented in Partial Fulfillment of the Requirements for graduation *with research distinction in
Astronomy* in the undergraduate colleges of The Ohio State University

by

Li-Wei Hung

The Ohio State University
March 2011

Project Adviser: Professor Andrew Gould, Scott Gaudi, and Richard Pogge; Department of
Astronomy

Searching for Extrasolar Planets in the Gravitational Microlensing Event MOA-2010-BLG-311

Li-Wei Hung¹

ABSTRACT

We analyze the microlensing event MOA-2010-BLG-311 that took place in June 2010. MOA-2010-BLG-311 has a high magnification ($A_{max} \sim 600$) with complete data coverage over the peak, making it very sensitive to planetary signals. The lightcurve, composed of observations from twelve observatories, is fitted by a single-lens model with finite-source effect. By looking at the residuals from the fit, we find no obvious planetary signals. The result can be confirmed with additional data that is currently being processed. In general, the probability of detecting a planet strongly depends on the planet mass, the planet separation from its parent star, and the angle of the source trajectory with respect to the binary axis. By simulating lightcurves and fitting them with single lens models, we constrain the range of planets that should be detected, if present, in this event.

Subject headings: Galaxy: bulge — gravitational lensing: micro — planetary systems: detection

1. Introduction

To date, more than five hundred extrasolar planets have been discovered, including numerous multiple-planet systems such as the recent detected six transiting planets orbiting around the Sun-like star Kepler-11 (Lissauer et al. 2011). These extrasolar planets and planet systems have an enormous range of properties unlike our own. By studying extrasolar planets, we hope to understand the planet formation, evolution, and the uniqueness of our own solar system. Among many current methods of searching for extrasolar planets, gravitational microlensing is an emerging technique made possible by recent advancements in technology.

Gravitational microlensing is a magnification phenomenon due to the effect of gravity. Gravitational microlensing occurs when a foreground star happens to pass close by a background star

¹The Ohio State University, Enarson Hall 154 W 12th Avenue, Columbus, OH 43210; hung.88@buckeyemail.osu.edu.

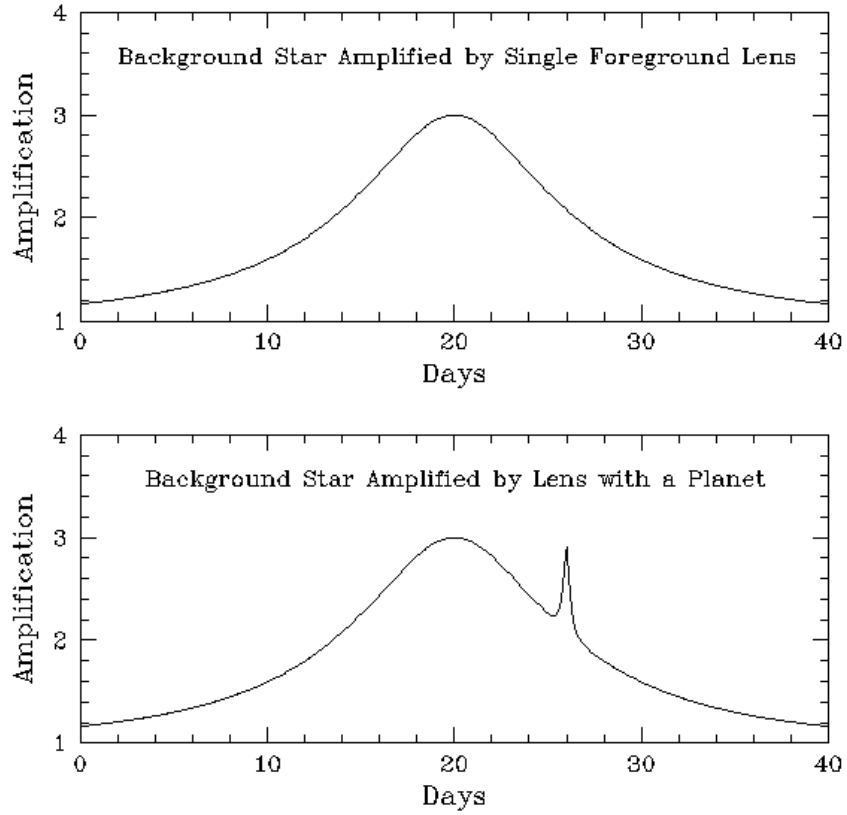


Fig. 1.— Example lightcurves of microlensing events. The top panel is the lightcurve produced by a single lens, i.e., assuming it has no planets. As the lens star passes in front of the source star, the brightness of the latter is magnified smoothly. The bottom panel shows the lightcurve in the presence of a planet. Since the planet acts like a small lens, it further magnifies the background star and leaves a sharp, short duration peak on top of the single lens the lightcurve. (*Source*: "The Search for Extra-Solar Planets by Microlensing." *PLANET Microlensing Collaboration Homepage*. Web. 03 Sept. 2010. <http://planet.iap.fr/planeet.html>.)

along our line of sight. The gravity of the foreground star bends the light rays from the background star and produces two unresolved images near a circle, named the Einstein ring. These images are magnified as the foreground star acts like a magnifying lens operating on the background star. When a lens star moves relative to a source star, the magnification of the source star varies with time; this is called a gravitational microlensing event. The corresponding brightness of the system is usually plotted as a function of time, known as a lightcurve. The top panel in Fig. 1 shows a typical microlensing lightcurve. The brightness of the system increases and then decreases, corresponding to two stars lining up and moving away relative to each other. A typical single lens lightcurve has a characteristic broad peak in the middle with smooth wings on the sides.

Extrasolar planets signals are detectable through a microlensing event by identifying small perturbations on the lightcurve caused by the planets. In a microlensing event, if the foreground star happens to host a planet, the system becomes a binary lens system; the foreground star acts like a major lens, where as the planet acts like a minor lens. Planetary signals become detectable if the position of the planet is near the Einstein ring at the time of the event. In this case, the gravity from the planet will further perturb the magnified images near the Einstein ring and create a short-lived deviation from a single lens lightcurve (Mao & Paczynski 1991; Gould & Loeb 1992). The bottom panel of Fig. 1 shows an example of a lightcurve that contains planetary signals. The small, sharp feature on the right side indicates the present of an extrasolar planet.

Gravitational microlensing can detect low-mass planets that would not otherwise be detected by any other method. Light from a star falls rapidly as the distance increases. Unlike other methods of detection, gravitational microlensing does not rely on detecting light from the planet or the host star directly. Therefore, it is capable of detecting Earth-mass planets and planets far away from the host stars. Ultimately, microlensing is potentially sensitive to multiple-planet systems similar to our solar system (except Mercury). By determining the demographics of planets throughout our Galaxy, gravitational microlensing will also provide a crucial test of planet formation theories (Gaudi 2010).

This thesis focuses on the microlensing event MOA-2010-BLG-311, which peaked in June 2010. This event is very sensitive to planetary signals for two reasons. First, the peak magnification of the event is $A_{max} \sim 600$. For such a high magnification event, the two magnified images spread through a wider range along the Einstein ring, making the detection less dependent on the angular position of the planet and thus greatly increasing the probability of detecting planets. Second, this event has the 4th complete data coverage over the peak where it is most sensitive to planetary signals. Together, the high magnification with complete data coverage makes MB10311 extremely sensitive to extrasolar planets.

In this thesis, we study the microlensing event MOA-2010-BLG-311. In § 2, we describe the observations acquired from 12 observatories and the data reduction. In § 3, we present our analysis

and results, including fitting the lightcurve to a single lens model with finite source-effect . In § 4, we analyze the sensitivity range and detection efficiency of this event for planets with various mass ratios. Finally, in § 5, we discuss the implications of our results and additional data available in the future.

2. Observations and Data Reduction

On 2010 June 15 ($\text{HJD}' \equiv \text{HJD} - 2450000 = 5362.967$), the Microlensing Observations in Astrophysics (MOA) collaboration detected a new microlensing event MOA-2010-BLG-310 at (R.A., decl.) = ($18^{\text{h}}08^{\text{m}}49^{\text{s}}.98$, $-25^{\circ}57'04.''27$) (J2000.0), along our line of sight toward the Galactic bulge. Within a day, this event was identified as likely to reach high magnification. Fig. 2 shows that the brightness of the star increases significantly, and it is easy to identify the lensing system by comparing images taken at different time. The Microlensing Follow Up Network (μFUN) then immediately began the intensive follow up observations.

The observational data were acquired from multiple observatories, including MOA, μFUN , and PLANET collaborations. In total, twelve observatories have observed the event for more than one night, and thus their data were used in the following analysis. Among these twelve observatories, eight of them are from μFUN : Auckland (AO, New Zealand), Bronberg (South Africa), CTIO SMARTS 1.3 meter (Chile), Farm Cove (FCO, New Zealand), Kumeu (New Zealand), Molehill (MAO, New Zealand), Vintage Lane (VLO, New Zealand), and Wise (Israel); three are from PLANET: SAAO, La Silla, and Liverpool; and one is from MOA.

In particular, observations from μFUN Bronberg and μFUN VLO provided the nearly complete coverage over the event peak between $\text{HJD}' = 5365.0$ and $\text{HJD}' = 5365.4$. Along with the Bronberg and VLO observations, MOA observations also covered the peak of the event. However, MOA observations near the peak (between $\text{HJD}' = 5365.10000$ and $\text{HJD}' = 5365.24000$) were not used for the analysis since the data shows strong deviations from a single-lens form that are not confirmed by contemporaneous data from other observatories.

The data from the μFUN observatories were reduced using the standard DoPhot reduction, with the exception of Bronberg and VLO data that were reduced using difference image analysis. Data from the PLANET collaboration were reduced using pySIS2 pipeline, and the MOA data were reduced with their standard pipeline. After the reduction, we exclude $> 3\sigma$ outliers. To avoid accidentally removing the planetary signals, we carefully examine these outliers by comparing observations taken at the same time from different observatories before excluding them. The uncertainties in each individual data set are normalized so that χ^2 per degree of freedom is close to unity. We bin the data with five different bin sizes according to the time the data were taken (Table

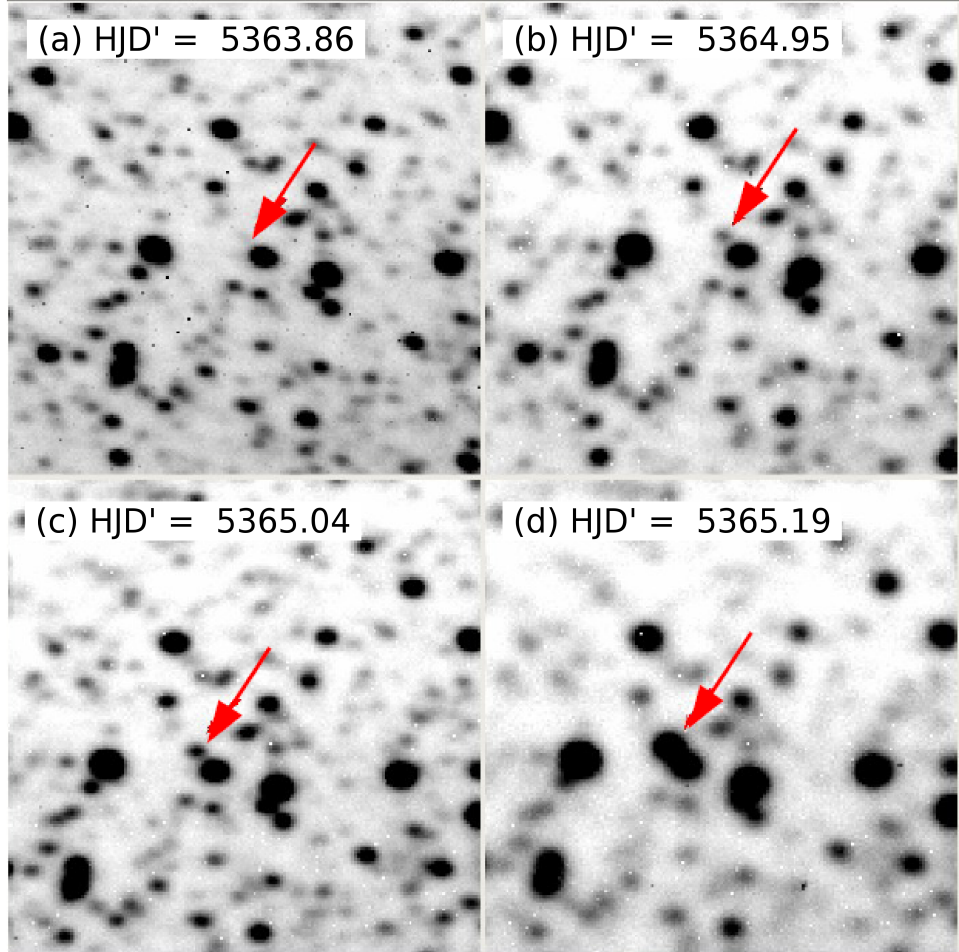


Fig. 2.— VLO images of the microlensing event MOA-2010-BLG-311. The maximum magnification A of this event is roughly 600. (a) The image was taken a day after MOA collaboration detected the event. The lensed star is barely detected. Images (b), (c), and (d) were taken on the same night, a few hours apart. The last image shows how bright the lensing system became near the peak of the event.

1).

3. Data Analysis and Results

3.1. Color-magnitude Diagram

We construct a color-magnitude diagram (CMD) of the field of view containing the lensing event (Fig. 3) to calibrate the source color. The CMD is derived from three CTIO V-band images and multiple I-band images near the peak. There are indeed four V-band images taken. However, only three of the images are of sufficient quality to contribute to the CMD. We visually checked each of the three images to make sure that there were no obvious defects such as cosmic rays in the images. In the top right hand side of the Fig. 3, a red dot at (0.40, 15.5) marks the center of the stars in a clump, called the red clump, which are metal-rich, helium burning stars. By assuming the color-magnitude distribution of the red clump stars is uniform across the Galactic bulge, we used the center of the red clump to calibrate the CMD. The black dot in the lower part of the Fig. 3 represents the source. The source has roughly the same color as the red clump.

3.2. Single-lens Model

MOA-2010-BLG-311 does not have obvious planetary signals, which was also the case for the event MOA-2008-BLG-310 (Janczak et al. 2010). However, Janczak et al. (2010) found a sub-Saturn-mass planet MOA-2008-BLG-310Lb by first looking at the residuals from fitting a single lens model. Fitting the well reduced observations with a single lensing model will give us an initial assessment whether there is a detectable planetary signal. Therefore, in this section, we focus on fitting the lightcurve to a single lens model with a finite-source effect. The lightcurve of

Table 1. Bin sizes used on MOA-2010-BLG-311

Time Block (HJD')	Bin Size (day)	Bin Size (min)
3658 - 5165	365	
5165 - 5340	30	
5340 - 5365.1	0.02	28.8
5365.1 - 5365.32	0.006	8.64
5365.32 - 5378	0.02	28.8

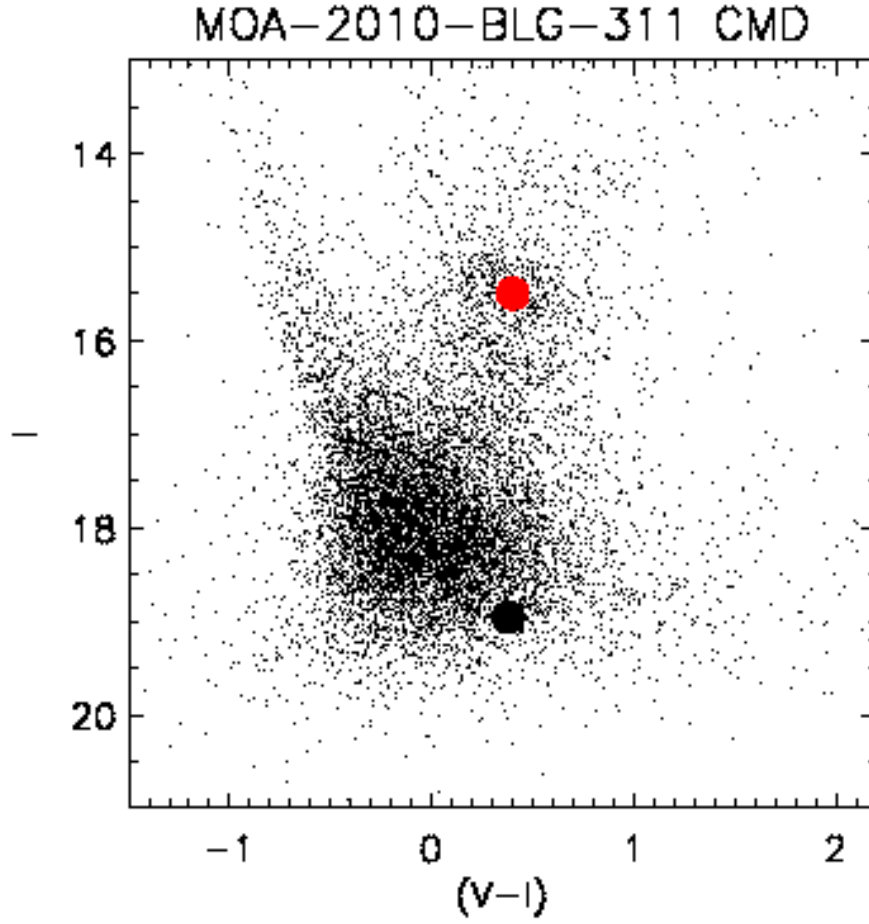


Fig. 3.— The color-magnitude diagram of the field of view of MOA-2010-BLG-311 constructed from the CTIO observations. The red circle on the top shows the center of the red clump (0.40, 15.5), where as the black circle at the bottom indicates the source (0.3786, 18.9561). Notice that the source has roughly the same color as the red clump.

MOA-2010-BLG-311 is shown in Fig. 4, and the best fit parameters are shown in Table 2.

3.2.1. Finite-source Effects

Ideally, if the lens star lines up perfectly with a point source, the magnification of the source star should be infinity. However, in a real microlensing event, the source is not a mathematical point. The finite projected area of the source star prevents the magnification from shooting up to infinity. The peak of an event is where the finite source effect becomes significant since the lens star and the source star are close together in projection. In MOA-2010-BLG-311, this finite-source effect was considered in the fit.

We need to consider the limb darkening of the source in order to fit the lightcurve with the finite-source effect. We first estimate the temperature of the source. When comparing the source position from Yee et al. (2009) to ours (Fig. 3), both sources occupied almost the same spot relative to the position of the red clumps on the CMDs, with our source being slightly redder. In Yee et al. (2009), the temperature of the source was determined to be 5250 K by fitting the isochrones. Thus, for the source temperature here, we estimate $T_{\text{eff}} \sim 5000$ K. Assuming a microturbulent velocity = 2 km s^{-1} , $\log g = 4.5$, solar metallicity, and $T_{\text{eff}} = 5000$ K, we found the limb-darkening coefficients to be $u_V = 0.7615$, $u_I = 0.5905$, and $u_H = 0.4055$ using the online data base provided by Claret (2000). u_V , u_I , and u_H are then converted to the linear limb-darkening parameter

$$\Gamma = \frac{2u}{3-u} \quad (1)$$

to obtain $\Gamma_V = 0.68$, $\Gamma_I = 0.49$, and $\Gamma_H = 0.31$. Keeping the limb-darkening parameters fixed, we found the best fit of the normalized source size to be $\rho_* = 3.97 \times 10^{-3}$.

The single lens model with finite source effect fits the observation well. In contrast to the event in Janczak et al. (2010), MOA-2010-BLG-311 does not have a clear deviation from a single lens model, especially near the peak of the event as marked with the black vertical lines in Fig. 4. Therefore, with our initial assessment on the currently available data, no planets have been detected in this event.

Table 2. Best Fit Parameters of the Lightcurve with the Finite-source Effect

t_0 (HJD')	u_0 (θ_E)	t_E (days)	ρ_* (θ_E)	Γ_V	Γ_I	Γ_H
5365.196719	0.002314	14.089261	0.003880	0.68 (fixed)	0.49 (fixed)	0.31 (fixed)

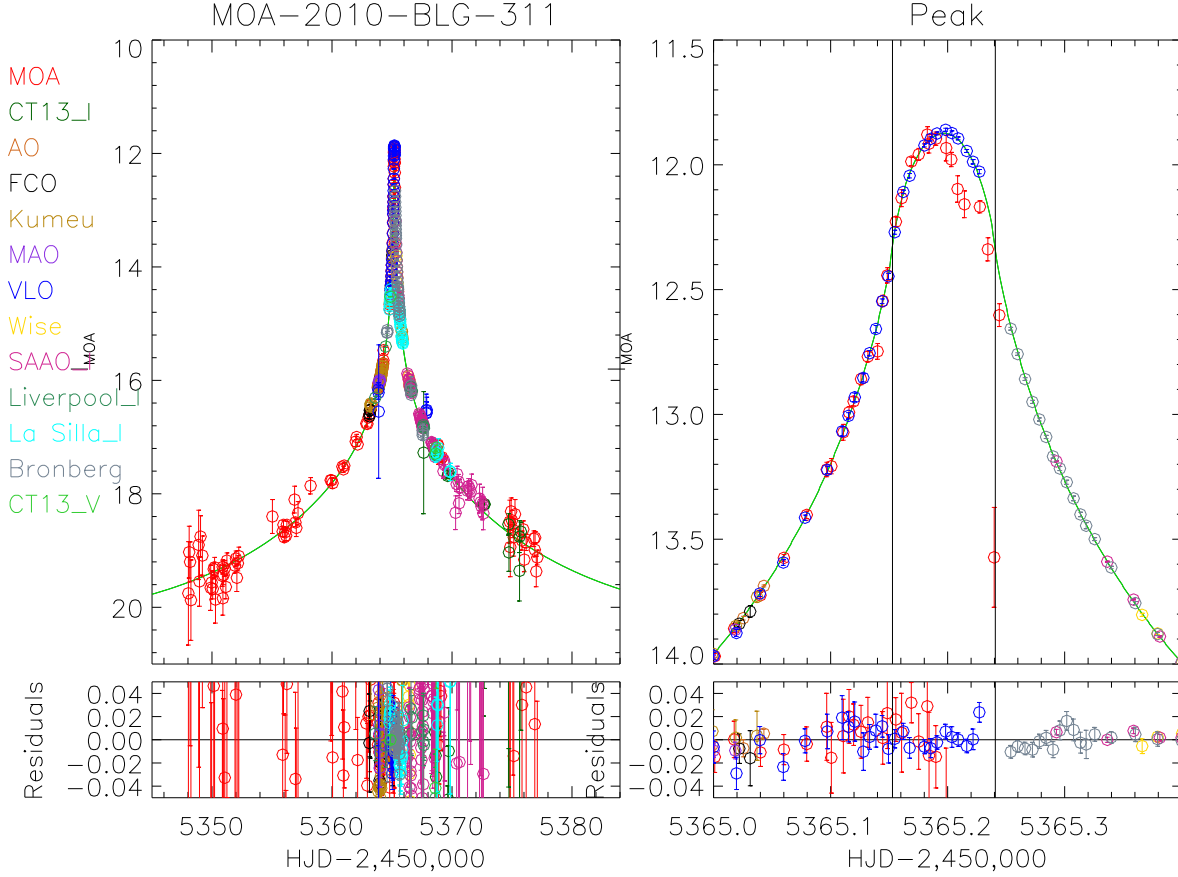


Fig. 4.— The lightcurve of MOA-2010-BLG-311. The entire event is shown in the left panel. The right panel shows an enlargement of the peak. The event was observed by several different observatories, as color-coded on the side. All the observations are rescaled to the MOA flux. The points are binned according to Table 1. The best fit single lens model with finite source effect is plotted as the green solid curve. Since the MOA data over the peak disagree with other simultaneous observations (probably due to instrumental effects), we exclude the MOA observations near the peak for the fit. The residuals from the fit are shown in the bottom two panels. The region between the black vertical lines on the right panel indicates the time period that is most sensitive to planetary signals. The small residuals suggest no detectable planetary signals.

3.3. Lens Proper Motion

Not many planets have been detected in both open and globular clusters. In the former case, current observations are insufficient to place a constraint on whether there is a fundamental difference between the frequency of planets in open clusters and in the field (van Saders & Gaudi 2010). The first planet detected in a globular cluster is PSR B1620-26 b (Backer et al. 1993). Inspired by the discovery, multiple projects had been designated to search for planets in globular clusters. Searching for transiting planets has been done on 47 Tucanae (Gilliland et al. 2000; Weldrake et al. 2007) and ω Centauri (Weldrake et al. 2007), but not a single planet was found. Fregeau et al. (2006) argues that the dynamics of the cluster is not the cause of the lack of planets in globular clusters since the encounter times are longer than the Hubble time for close planets. Instead, low stellar metallicity in globular clusters is the dominate limiting factor on the frequency of planets (Weldrake et al. 2007). Nonetheless, Debes & Jackson (2010) argues that more planets with low mass and long orbits can be detected in the globular clusters once a large number of the transiting targets are observed.

When the follow up observations were taken for MOA-2010-BLG-311, several observers noticed the microlensing event was projected close to the globular cluster NGC 6553. Fig. 5 shows the relative distance between the event and the cluster. The close proximity of the event to the cluster raises the interesting possibility that MOA-2010-BLG-311 might be the first microlensing event involving a globular cluster member. If the previous statement is true, the result of the analysis would contribute to characterizing the frequency of planets in globular clusters.

Whether the lens star is a member of the cluster can be identified by calculating the proper motion of the lens star. We use the corrected $V - I$ color of the source from CTIO observations to obtain the surface brightness by adopting the relation derived by Kervella et al. (2004). Then, combining the corrected I magnitude with this surface brightness yields the angular source size $\theta_\star = 1.58 \mu\text{as}$. The angular source size θ_\star , normalized source size ρ_\star , and the Einstein ring radius θ_E are related by

$$\theta_E = \frac{\theta_\star}{\rho_\star}. \quad (2)$$

With $\theta_\star = 1.58 \mu\text{as}$, and $\rho_\star = 3.97 \times 10^{-3}$, we find $\theta_E = 0.41 \text{ mas}$. The proper motion μ of the lens is given by

$$\mu = \frac{\theta_E}{t_E} = 10.5 \text{ mas yr}^{-1}. \quad (3)$$

Considering the fast proper motion of 10.5 mas yr^{-1} of the lens star, it is unlikely that the lens

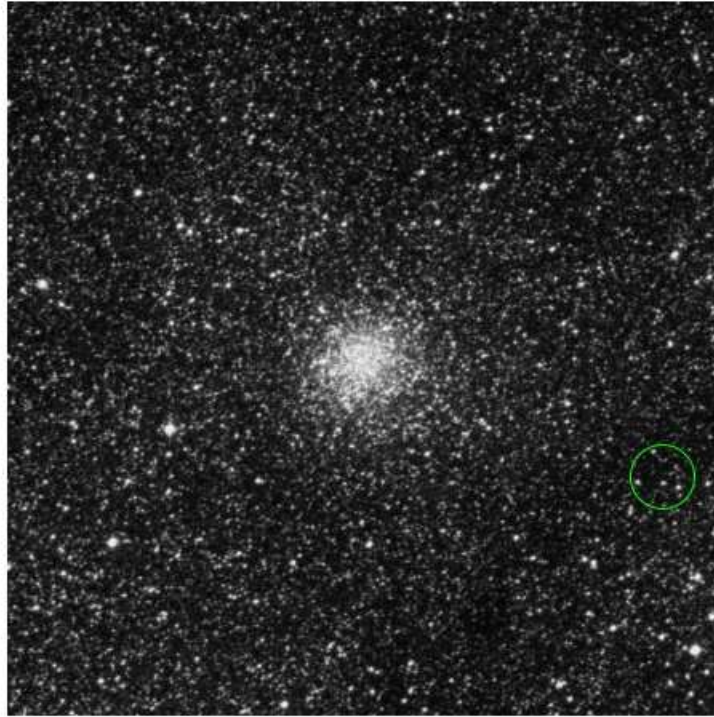


Fig. 5.— The position of the source star relative the nearby globular cluster NGC 6553. The green circle indicates the position of the microlensing event. Because there is a globular cluster near the event, the lens star might be a member of the cluster. However, the proper motion of the lens is fast (~ 10.6 mas/yr), which makes it unlikely to be a member of the cluster.

is a member of the globular cluster.

4. Event Sensitivity

In order to address our conclusion scientifically, we need to analyze what is the detection limitation specifically for this event. We must analyze the sensitivity range of each microlensing event individually because the probability of detecting planets varies. The probability of detecting planets increases as the magnification increases. Since in a high magnification event, the unresolved source images cover a larger portion of the Einstein ring, a planet has a higher probability to perturb the images. In addition, for high magnification event, the probability increases linearly as the planet mass (Gaudi 2010) since a larger planet is expected to create a larger signal. The probability also depends on a planet’s position during the time of the event because the planet must be near one of the two magnified images near the Einstein ring where the perturbation becomes detectable. As a result, detection through gravitational microlensing is biased toward large planets near the Einstein rings in high magnification events. These parameters, such as the magnification and the geometry of the systems, are different for each event. Therefore, to characterize the detection probability, we must analyze each event individually.

The sensitivity range for an event is analyzed with synthetic lightcurves. The times at which the observations were made with the associated error bars on the real measurements are fed into an existing FORTRAN program written by Dr. S. Dong and J. Yee of the Ohio State Astronomy Department. This program simulates a lightcurve assuming there is a planet with a certain mass and position at the time of the event. The input mass and position of the planet are controlled variables. Then, the single lens model is used to fit the synthesized lightcurve to determine the corresponding χ^2 . A large χ^2 indicates the input mass and position of a planet are strong enough to create a significant deviation from a single lens model, and thus the planet with those parameters are detectable.

About 17,500 synthesized lightcurves with different combinations of mass ratio and planet position are fit with the single lens model for the event. Four different planet to star mass ratios are considered here: $q = 10^{-3}$, 10^{-4} , 10^{-5} , and 10^{-6} . For comparison, Jupiter has a mass ratio of about 10^{-3} , whereas the Earth has a mass ratio in the order of magnitude of $10^{-5.5}$. Such analysis maps out the complete detection probability for each scenario as shown in Fig. 6. Note that the detectable zone (blue) is much larger for larger mass ratios. This result can be understood since a planet with a larger mass ratio is expected to create a stronger disturbance on the lightcurve and thus it is more easily detected.

Based on the simulation results, we also generate a plot with mass ratio and separation as x and

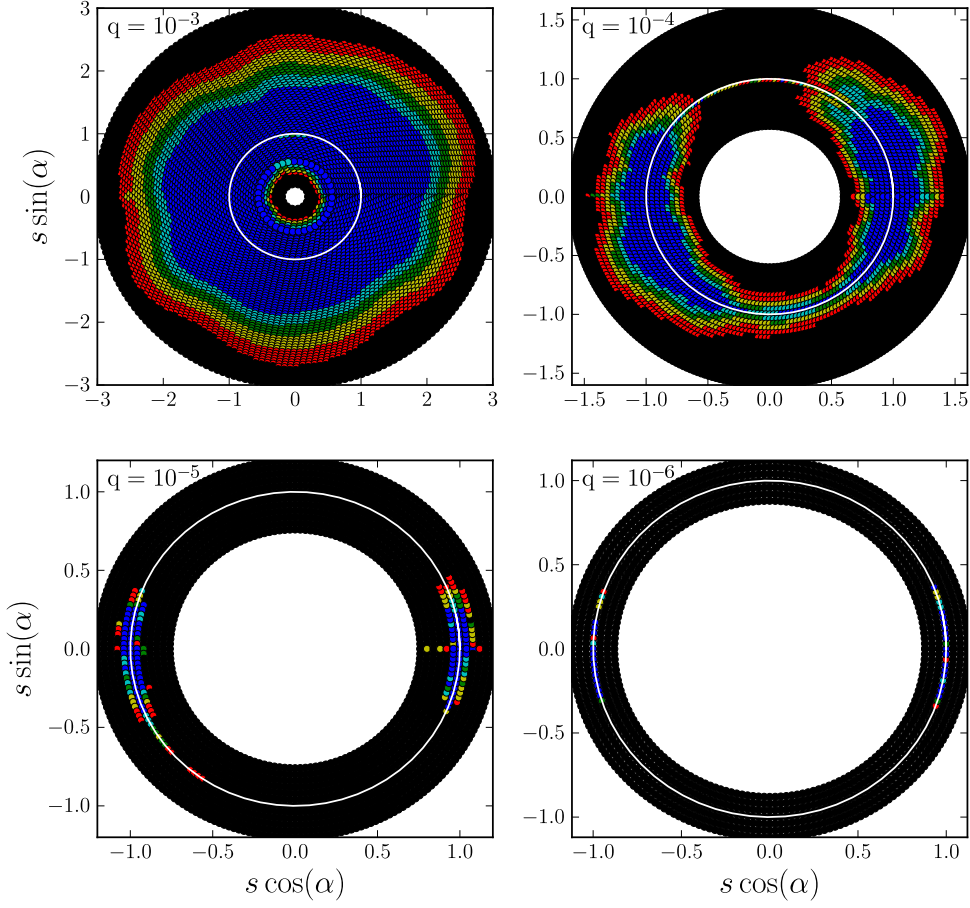


Fig. 6.— The sensitivity map of the event. The four different panels show the face on view of sensitivity range of the system with different mass ratio q . The white circles indicate the position of the Einstein rings. Blue, cyan, green, yellow, red, and black correspond to the $\Delta\chi^2$ values of > 400 , $400-250$, $250-160$, $160-100$, $100-60$, and < 60 . As expected, the area near the Einstein ring has higher probability to detect planets. Note how as a planet becomes larger (large q), the detectable area increases.

y axes verses probability represented in different colors as shown in Fig. 7. The blue color indicates the region with high probability of detecting the planet, whereas the detection probability is low in the red region. Such analysis is important for further studies in understanding the frequency of solar like systems as discussed in detailed in Gould et al. (2010).

5. Discussion

The analysis showed no obvious detectable planetary signals in MOA-2010-BLG-311 as the preliminary result. The lightcurve of the microlensing event can be well described by a single lens model with finite-source effect. The lensing system is close in projection to a globular cluster. However, the lens star is calculated to have a high proper motion of 10.5 mas yr^{-1} , which makes it unlikely to be a member of the cluster. The sensitivity range of the event is also analyzed. The sensitivity and efficiency maps are show in Fig. 6 and Fig. 7. As expected, a high mass planet near the Einstein ring during the event has a high probability to be detected.

Even though no detectable planets have been found, a better conclusion can be reached with additional data and the rereduced MOA data. As mentioned in § 2, MOA data over the peak do not agree with observations taken at the other observatories. As a result, part of the MOA data is excluded in this analysis. Performing cameo reduction on the MOA data may improve the analysis result since the data over the peak of the event is most sensitive to planetary signals. There are additional observations from Arizona, South African, and Tasmania on MOA-2010-BLG-311, but they are currently not available due to the reduction problems. These additional data also include the *V*-band images close to the peak. If the data are successfully reduced, the *V*-band observations might be used to verify the color of the source obtained from the CTIO observations.

Acknowledgments

I acknowledge the NASA μ FUNgrant 1277721 for providing the initial training; the OSU Summer Undergraduate Research Program in Astrophysics for supporting the initiation of the project; and the Arts and Sciences Honors program for making the completion possible. I am grateful to Jennifer Yee and Andy Gould for advising through out the entire project. I am also thankful for Richard Pogge in assisting me in data reduction and Scott Gaudi for helpful discussions.

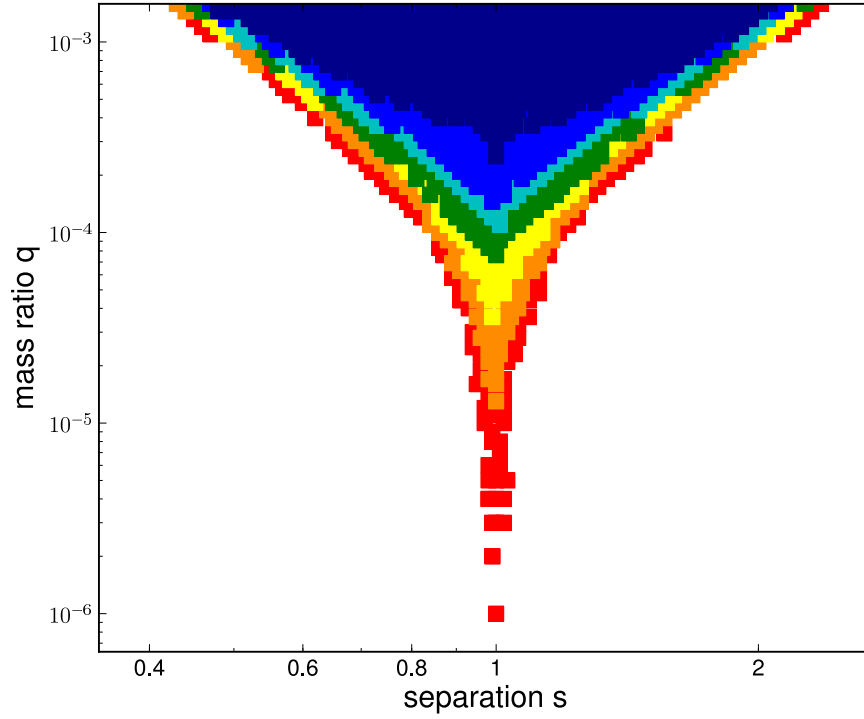


Fig. 7.— The triangle detection efficiency diagram in the mass ratio and separation log-log plot, assuming the planet is detectable when $\Delta\chi^2 > 400$. Separation has units of θ_E . Starting from the dark blue to red, the detection efficiency decreases from 100% to 0% with the decrement of 12.5%. Note that the detection efficiency is highest near the Einstein ring ($s = 1$). Also, as the mass ratio of the planet to the star increases, the detectable zone increases.

REFERENCES

- Backer, D. C., Foster, R. S., & Sallmen, S. 1993, *Nature*, 365, 817
- Claret, A. 2000, *A&A*, 363, 1081
- Debes, J. H. & Jackson, B. 2010, *ApJ*, 723, 1703
- Fregeau, J. M., Chatterjee, S., & Rasio, F. A. 2006, *ApJ*, 640, 1086
- Gaudi, B. S. 2010, ArXiv e-prints
- Gilliland, R. L., Brown, T. M., Guhathakurta, P., Sarajedini, A., Milone, E. F., Albrow, M. D., Baliber, N. R., Bruntt, H., Burrows, A., Charbonneau, D., Choi, P., Cochran, W. D., Edmonds, P. D., Frandsen, S., Howell, J. H., Lin, D. N. C., Marcy, G. W., Mayor, M., Naef, D., Sigurdsson, S., Stagg, C. R., Vandenberg, D. A., Vogt, S. S., & Williams, M. D. 2000, *ApJ*, 545, L47
- Gould, A., Dong, S., Gaudi, B. S., Udalski, A., Bond, I. A., Greenhill, J., Street, R. A., Dominik, M., Sumi, T., Szymański, M. K., Han, C., Allen, W., Bolt, G., Bos, M., Christie, G. W., DePoy, D. L., Drummond, J., Eastman, J. D., Gal-Yam, A., Higgins, D., Janczak, J., Kaspi, S., Kozłowski, S., Lee, C., Mallia, F., Maury, A., Maoz, D., McCormick, J., Monard, L. A. G., Moorhouse, D., Morgan, N., Natusch, T., Ofek, E. O., Park, B., Pogge, R. W., Polishook, D., Santallo, R., Shporer, A., Spector, O., Thornley, G., Yee, J. C., μ FUN Collaboration, Kubiak, M., Pietrzyński, G., Soszyński, I., Szewczyk, O., Wyrzykowski, Ł., Ulaczyk, K., Poleski, R., OGLE Collaboration, Abe, F., Bennett, D. P., Botzler, C. S., Douchin, D., Freeman, M., Fukui, A., Furusawa, K., Hearnshaw, J. B., Hosaka, S., Itow, Y., Kamiya, K., Kilmartin, P. M., Korpela, A., Lin, W., Ling, C. H., Makita, S., Masuda, K., Matsubara, Y., Miyake, N., Muraki, Y., Nagaya, M., Nishimoto, K., Ohnishi, K., Okumura, T., Perrott, Y. C., Philpott, L., Rattenbury, N., Saito, T., Sako, T., Sullivan, D. J., Sweatman, W. L., Tristram, P. J., von Seggern, E., Yock, P. C. M., MOA Collaboration, Albrow, M., Batista, V., Beaulieu, J. P., Brilliant, S., Caldwell, J., Calitz, J. J., Cassan, A., Cole, A., Cook, K., Coutures, C., Dieters, S., Dominis Prester, D., Donatowicz, J., Fouqué, P., Hill, K., Hoffman, M., Jablonski, F., Kane, S. R., Kains, N., Kubas, D., Marquette, J., Martin, R., Martioli, E., Meintjes, P., Menzies, J., Pedretti, E., Pollard, K., Sahu, K. C., Vinter, C., Wambsganss, J., Watson, R., Williams, A., Zub, M., PLANET Collaboration, Allan, A., Bode, M. F., Bramich, D. M., Burgdorf, M. J., Clay, N., Fraser, S., Hawkins, E., Horne, K., Kerins, E., Lister, T. A., Mottram, C., Saunders, E. S., Snodgrass, C., Steele, I. A., Tsapras, Y., RoboNet Collaboration, Jørgensen, U. G., Anguita, T., Bozza, V., Calchi Novati, S., Harpsøe, K., Hinse, T. C., Hundertmark, M., Kjærgaard, P., Liebig, C., Mancini, L., Masi,

- G., Mathiasen, M., Rahvar, S., Ricci, D., Scarpetta, G., Southworth, J., Surdej, J., Thöne, C. C., & MiNDSTeP Consortium. 2010, *ApJ*, 720, 1073
- Gould, A. & Loeb, A. 1992, *ApJ*, 396, 104
- Janczak, J., Fukui, A., Dong, S., Monard, L. A. G., Kozłowski, S., Gould, A., Beaulieu, J. P., Kubas, D., Marquette, J. B., Sumi, T., Bond, I. A., Bennett, D. P., Abe, F., Furusawa, K., Hearnshaw, J. B., Hosaka, S., Itow, Y., Kamiya, K., Korpela, A. V., Kilmartin, P. M., Lin, W., Ling, C. H., Makita, S., Masuda, K., Matsubara, Y., Miyake, N., Muraki, Y., Nagaya, M., Nagayama, T., Nishimoto, K., Ohnishi, K., Perrott, Y. C., Rattenbury, N. J., Sako, T., Saito, T., Skuljan, L., Sullivan, D. J., Sweatman, W. L., Tristram, P. J., Yock, P. C. M., The MOA Collaboration, An, J. H., Christie, G. W., Chung, S., DePoy, D. L., Gaudi, B. S., Han, C., Lee, C., Mallia, F., Natusch, T., Park, B., Pogge, R. W., The μ FUN Collaboration, Anguita, T., Calchi Novati, S., Dominik, M., Jørgensen, U. G., Masi, G., Mathiasen, M., The MiNDSTeP Collaboration, Batista, V., Brilliant, S., Cassan, A., Cole, A., Corrales, E., Coutures, C., Dieters, S., Fouqué, P., Greenhill, J., & The PLANET Collaboration. 2010, *ApJ*, 711, 731
- Kervella, P., Thévenin, F., Di Folco, E., & Ségransan, D. 2004, *A&A*, 426, 297
- Lissauer, J. J., Fabrycky, D. C., Ford, E. B., Borucki, W. J., Fressin, F., Marcy, G. W., Orosz, J. A., Rowe, J. F., Torres, G., Welsh, W. F., Batalha, N. M., Bryson, S. T., Buchhave, L. A., Caldwell, D. A., Carter, J. A., Charbonneau, D., Christiansen, J. L., Cochran, W. D., Desert, J., Dunham, E. W., Fanelli, M. N., Fortney, J. J., Gautier, III, T. N., Geary, J. C., Gilliland, R. L., Haas, M. R., Hall, J. R., Holman, M. J., Koch, D. G., Latham, D. W., Lopez, E., McCauliff, S., Miller, N., Morehead, R. C., Quintana, E. V., Ragozzine, D., Sasselov, D., Short, D. R., & Steffen, J. H. 2011, *Nature*, 470, 53
- Mao, S. & Paczynski, B. 1991, *ApJ*, 374, L37
- van Saders, J. L. & Gaudi, B. S. 2010, ArXiv e-prints
- Weldrake, D. T. F., Sackett, P. D., & Bridges, T. J. 2007, in *Astronomical Society of the Pacific Conference Series*, Vol. 366, *Transiting Extrapolar Planets Workshop*, ed. C. Afonso, D. Weldrake, & T. Henning, 289–+
- Yee, J. C., Udalski, A., Sumi, T., Dong, S., Kozłowski, S., Bird, J. C., Cole, A., Higgins, D., McCormick, J., Monard, L. A. G., Polishook, D., Shporer, A., Spector, O., Szymański, M. K., Kubiak, M., Pietrzyński, G., Soszyński, I., Szewczyk, O., Ulaczyk, K., Wyrzykowski, Ł., Poleski, R., The OGLE Collaboration, Allen, W., Bos, M., Christie, G. W., DePoy, D. L., Eastman, J. D., Gaudi, B. S., Gould, A., Han, C., Kaspi, S., Lee, C., Mallia, F., Maury, A.,

Maoz, D., Natusch, T., Park, B., Pogge, R. W., Santallo, R., The μ FUN Collaboration, Abe, F., Bond, I. A., Fukui, A., Furusawa, K., Hearnshaw, J. B., Hosaka, S., Itow, Y., Kamiya, K., Korpela, A. V., Kilmartin, P. M., Lin, W., Ling, C. H., Makita, S., Masuda, K., Matsubara, Y., Miyake, N., Muraki, Y., Nagaya, M., Nishimoto, K., Ohnishi, K., Perrott, Y. C., Rattenbury, N. J., Sako, T., Saito, T., Skuljan, L., Sullivan, D. J., Sweatman, W. L., Tristram, P. J., Yock, P. C. M., The MOA Collaboration, Albrow, M. D., Batista, V., Fouqué, P., Beaulieu, J., Bennett, D. P., Cassan, A., Comparat, J., Coutures, C., Dieters, S., Greenhill, J., Horne, K., Kains, N., Kubas, D., Martin, R., Menzies, J., Wambsganss, J., Williams, A., Zub, M., & The PLANET Collaboration. 2009, ApJ, 703, 2082